

Material Dependence of NBTI Physical Mechanism in Silicon Oxynitride (SiON) p-MOSFETs: A Comprehensive Study by Ultra-Fast On-The-Fly (UF-OTF) I_{DLIN} Technique

E. N. Kumar, V. D. Maheta, S. Purawat, A. E. Islam¹, C. Olsen², K. Ahmed², M. A. Alam¹ and S. Mahapatra

Department of Electrical Engineering, IIT Bombay, India (Email: souvik@ee.iitb.ac.in, Ph:+91-22-25720408, Fax:+91-22-25723707)

¹School of EECS, Purdue University, W. Lafayette, IN, USA, ²Applied Materials, Santa Clara, CA, USA

ABSTRACT

An Ultra-Fast On-The-Fly (UF-OTF) I_{DLIN} technique having 1 μ s resolution is developed and used to study gate insulator process dependence of NBTI in Silicon Oxynitride (SiON) p-MOSFETs. The Nitrogen density at the Si-SiON interface and the thickness of SiON layer are shown to impact temperature, time, and field dependencies of NBTI. The plausible material dependence of NBTI physical mechanism is explored.

INTRODUCTION AND BACKGROUND

Negative Bias Temperature Instability (NBTI) is a serious reliability issue for SiON p-MOSFETs [1-8]. It is important to understand the physical mechanism of NBTI, i.e., whether it is dominated by generation of interface traps (ΔN_{IT}) [3,4] or by hole trapping in pre-existing traps (ΔN_h) [1,2,5,6], to develop proper models [5-7,9-12] to extrapolate stress data (high V_G , short time) to operating (low V_G , long time) condition. Using Ultra-Fast Stress-Measure-Stress (UF-SMS) scheme [7], it has recently been suggested that NBTI is purely a ΔN_h related effect. Therefore, conclusions based on relatively slower, conventional On-The-Fly (C-OTF) method [13]; i.e., ΔN_{IT} dominates NBTI in plasma nitrided oxides (PNO), and both ΔN_{IT} and ΔN_h contribute in thicker thermal nitrided oxides (TNO) [8], need to be re-verified. As reliable lifetime extrapolation depends on the mechanics of ΔN_h and/or ΔN_{IT} dependence of NBTI degradation, it is important to reconsider all older results by ultra-fast measurements.

In this work, an UF-OTF scheme (see Fig.1) is used to study the time, temperature (T) and field (E_{OX}) dependence of NBTI in SiON p-MOSFETs having different N profile, N density and film thickness (see Table-1). It is shown that the Si-SiON interfacial N density and SiON thickness determine the time exponent (n), T activation (E_A) and E_{OX} -dependence (Γ) of NBTI, re-verifying previous conclusions [8]. Plausible process dependence of ΔN_{IT} and ΔN_h contribution to overall NBTI is suggested. Such material dependence of NBTI has not been appreciated by recent modeling attempts [5-7,9-12], and must be considered for reliable lifetime estimation.

TIME DEPENDENCE

Under identical stress E_{OX} and T, TNO (in spite having lower total N dose) shows much larger I_{DLIN} degradation than PNO (Fig.2). The extracted degradation (Fig.3) for TNO is not only larger, but also is significantly impacted by t_0 delay (time between application of stress V_G and I_{D0} measurement [14]). Note, extracted degradation (Fig.3) is related, but not exactly equal to V_T shift since mobility degradation is not separated [15]. In a log-log plot (Fig.2), TNO clearly shows much lower n (long time stress, for $t > 10s$) than PNO for all t_0 (Fig.4). Though n increases with higher t_0 as expected [14], for a given t_0 it remains constant for a large range of stress V_G and T (Fig.5), and indicates the robustness of the underlying

physical mechanism that governs time dependence of NBTI. For t_0 range of 1 μ s to $\sim 100\mu$ s, the observed variation in n is small (Fig.4) and well within the error bar caused by noise in I_{D0} measurement. As n saturates with reduction in t_0 , a faster ($t_0 < 1\mu$ s) OTF is not likely to produce much different values than reported with $t_0 = 1\mu$ s. Furthermore, lower n obtained for UF-OTF results in longer extrapolated lifetime than C-OTF (not shown), especially in PNO devices where the impact of t_0 on long-time degradation magnitude is small (Fig.3, LHS).

TNO shows (PNO does not show) log time dependence when plotted in a semi-log scale (Fig.6), as reported also in [2]. However, such log time dependence is not observed for thinner TNO and PNO (not shown). Even for thick TNO, the non-uniqueness of log-time dependent slope (as stress V_G and T are varied, not shown) makes it difficult to use it as reliable time extrapolation scheme. However when degradation is plotted as power-law time dependence, the robustness of n for long stress ($t > 10s$) holds for a wide range of stress V_G and T (n actually reduces slightly, by less than 0.01 for additional 2 decades in stress time due to reduction in stress E_{OX} [14]). This is true for a wide variety of devices studied (see Table-I) and makes power-law time dependence physically justified for extrapolation to end-of-life.

TEMPERATURE AND BIAS DEPENDENCE

PNO shows clear T dependence for the entire duration of stress (Fig.7, LHS). TNO shows larger overall degradation than PNO for all T, negligible T dependence at early stress time (up to $t \sim 1-10ms$), and weaker T dependence (compared to PNO) at longer stress time (Fig.7, RHS). Note, the overall difference in long-time degradation between TNO and PNO can be attributed to a large extent to the early, T independent degradation for TNO. For both PNO and TNO, long time T dependence follows Arrhenius activation, as is apparent from the T independence of n (Fig.5, LHS) [3]. Note that such T independence of n has been observed for all devices used in this study (not shown), irrespective of N dose, device type or EOT (as described in Table-I).

TNO shows higher degradation magnitude over a wide range of stress E_{OX} , but much lower Γ compared to PNO (Fig.8). For all E_{OX} , the difference in degradation magnitude as t_0 is varied (fixed t-stress) is much larger (the difference is more apparent at shorter stress time) for TNO compared to PNO. However for both PNO and TNO, Γ is independent of t_0 and stress time. Note, lower Γ for TNO results in higher degradation magnitude and lower lifetime as extrapolation is done from stress to operating E_{OX} (not shown).

PROCESS DEPENDENCE

Si-SiON interfacial N density is much larger for TNO compared to PNO for a particular total N dose [16,17]. The significantly different magnitude, time exponent, E_{OX} and T

dependence of degradation (see Figs.2-8) when PNO (D4) is compared to TNO (D7) can be attributed to differences in N density at Si-SiON interface (as XPS thicknesses are similar). This is verified with observed reduction in n , E_A and Γ as Si-SiON interfacial N density is increased, i.e., when D3 (PNO) is compared to and D5 (TNO+PNO) and D6 (TNO) having similar XPS thickness (Fig.9). It is interesting to note that in spite of having drastically different N profile (Fig.10, top) and very different N density at the SiON-poly-Si interface, similar Si-SiON interfacial N density for D5 and D6 results in nearly identical NBTI magnitude (not shown), n , E_A and Γ . This shows that N density at SiON-poly-Si interface does not play a significant role in NBTI. Therefore, though D4 has higher total N dose and higher N density at the SiON-poly-Si interface compared to D7, higher N density at the Si-SiON interface for the later results in higher NBTI (see Figs.3,6,7).

For PNO, NBTI magnitude increases (not shown), while n , E_A and Γ reduces as total N dose is increased (D1 to D2), or as total N dose is increased while XPS thickness is reduced (D4 to D2), consistent with increase in Si-SiON interfacial N density. However, note that the above process changes caused a drastic increase in atomic N% (16% for D4, 22% for D1 but 41% for D2) and significant increase in Si-SiON interfacial N density. For PNO having small N dose, Γ reduces slightly but n and E_A remain constant as XPS thickness is reduced (D4 to D1). For TNO, n and E_A increases but Γ remains constant as XPS thickness is reduced at constant N dose (D7 to D6).

PHYSICAL MECHANISM

It is believed that NBTI is due to donor like ΔN_{IT} [3,4] and/or ΔN_h [1,2]. Tunneling of inversion layer holes (depends on hole density, tunneling barrier and E_{OX}) to Si-H bonds at the Si-SiON interface and N-related trap sites in SiON bulk respectively results in ΔN_{IT} and ΔN_h (illustrated in Fig.10, bottom). ΔN_{IT} shows power law time dependence and strong T activation [3,4,8,11]. Nature of diffusion species (released from broken Si-) determines n . Classical diffusion suggests $n=0.5$ for H^+ , $=0.25$ for H^0 , $=0.16$ for H_2 (T independent) [10, 18]. Dispersive diffusion suggests $n \leq 0.5$ for H^+ , ≤ 0.25 for H^0 , ≤ 0.16 for H_2 with T dependent n [12,19]. ΔN_h shows log time dependence and weak T activation [1,2]. The N density at Si-SiON interface impacts hole tunneling barrier [11] and Si-H bond strength [20] and therefore both ΔN_{IT} and ΔN_h . The N density at SiON bulk governs N-related trap sites and only ΔN_h . However, ΔN_h is more efficient near Si-SiON interface especially for thicker SiON due to higher tunnel in (from substrate) and lower tunnel out (to poly-Si) probabilities (see Fig.10, bottom). Generation of both N_{IT} (stronger time and T dependence) and N_h (weaker time and T dependence) would reduce the n and E_A of overall ΔV_T during NBT stress [8].

Unless N dose is high, NBTI in PNO (devices treated with proper *Post Nitridation Anneal*; have lower N density at Si-SiON interface) is likely dominated by ΔN_{IT} , as evident from clear T activation for entire stress duration (Fig.7, LHS), relatively higher and thickness independent n and E_A (Fig.9;

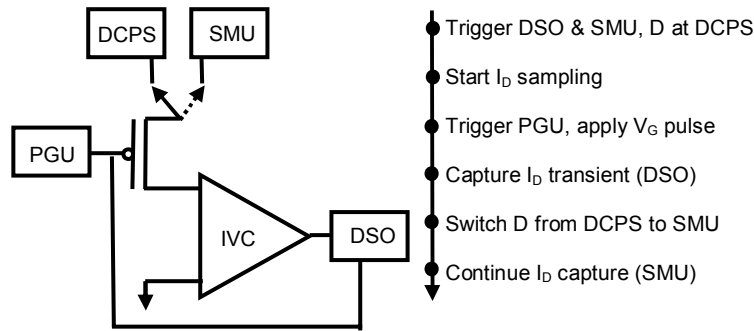
D1,D4). However as n is independent of T (Fig.5, RHS), the slightly lower n (~ 0.12) than predicted by basic theory (with H_2) is unlikely due to strong dispersive diffusion [12,19] and needs attention. Increase in total N dose results in higher N density at (or near) Si-SiON interface ($D2 > D3 > D1, D4$), and resultant reduction in n and E_A is possibly due to additional ΔN_h contribution (though ΔN_{IT} also increases [11,20]). As Si-SiON interfacial N density is very high for TNO (D6,D7) and TNO+PNO (D5), the contribution due to ΔN_h is significant and large reduction is observed in n and E_A (see Fig.9). In spite of similar interfacial N density for D6 and D7, lower tunnel out probability (see Fig.10, bottom) and higher charge trapping volume for the later cause higher ΔN_h and lower n and E_A . Unlike D4, NBTI in D7 is likely dominated by ΔN_h as evident from very high, T independent degradation at early stress time (Fig.7, RHS), log time dependence (Fig.6, RHS) [1,2] and very low n and E_A for long time ($t > 10s$) stress (see Fig.9). However, the time constant and T (in)dependence of ΔN_h needs careful attention to explain the T independence of n at longer stress time. Finally, Si-SiON interfacial N density similarly influences the E_{OX} dependence of ΔN_{IT} and ΔN_h by influencing the hole tunneling barrier, and hence Γ (though reduces for higher N density) is independent of t_0 and stress time (see Fig.8).

CONCLUSION

Using an UF-OTF technique, NBTI is studied in SiON p-MOSFETs having wide range of N density, N profile and SiON thickness. Measured NBTI parameters (n , Γ and E_A) show strong dependence on Si-SiON interfacial N density and film thickness. Experimental results are explained by process dependence of relative ΔN_{IT} and ΔN_h contribution to overall NBTI. In general, material dependence results from UF-OTF are consistent with that obtained earlier by C-OTF.

References:

- [1] V. Huard et al., p.40, IRPS 2004
- [2] M. Denais et al., p.109, IEDM 2004
- [3] D. Varghese et al., p.684, IEDM 2005
- [4] A. T. Krishnan et al., p.688, IEDM 2005
- [5] T. Yang et al., p.92, VLSI 2005
- [6] H. Reisinger et al., p.448, IRPS 2006
- [7] C. Shen et al., p. 12.5.1, IEDM 2006
- [8] S. Mahapatra et al., p.1, IRPS 2007
- [9] M. A Alam, p.345, IEDM 2003
- [10] S. Chakravarthi, p.273, IRPS 2004
- [11] A. E. Islam et al., p.12.4.1, IEDM 2006
- [12] T. Grasser et al., p.268, IRPS 2007
- [13] S. Rangan et al., p.341, IEDM 2003
- [14] A. E. Islam et al., APL, v.90, 083505, 2007
- [15] A. E. Islam et al., IEDM 2007
- [16] J. R. Shallenberger et al., JVST-A, v.17, p.1086, 1999.
- [17] S. Rauf et al., JAP, v.98, 024305, 2005.
- [18] M. A. Alam, NBTI Tutorial, IRPS 2006
- [19] B. Kaczer et al., p.381, IRPS 2005
- [20] S. S. Tan et al., SSDM, p.70, 2003.



D	Type	Base	N	XPS	EOT
1	PNO	15	2.8	18.5	14.0
2	PNO	15	5.8	21.0	12.3
3	PNO	20	5.3	23.2	15.6
4	PNO	25	3.1	28.1	23.5
5	TNO+ PNO	20	0.8+ 5.1	22.8	13.1
6	TNO	20	0.8	21.1	18.5
7	TNO	25	0.8	26.1	22.0

Fig.1. Ultra-Fast On-The-Fly (UF-OTF) I_{DLIN} setup and measurement sequence during NBTI stress. Initial I_{DLIN} transient ($1\mu s$ to $30ms$) is captured using IV Converter-DSO at S, with DC Power Supply at D. Long time I_{DLIN} transient is captured using SMU at D. Use of DCPS helps prevent RC related issues that affect I_{DLIN} transients in early time. IV converter is set for a gain of $10^3 - 10^4$.

Table-I. Process details of devices used. Starting oxide (Base), XPS thickness and EOT are in \AA , Nitrogen dose (N) in 10^{15} cm^{-2} . PNO: Plasma Nitrided Oxide, TNO: Thermal Nitrided Oxide. D4 and D7 are used in Figs. 2 through Fig.8.

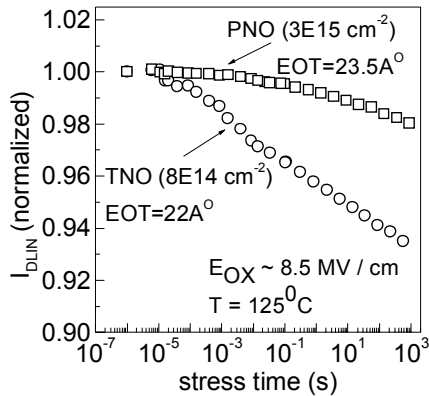


Fig.2. Captured I_{DLIN} transients for 9 decades of stress time for PNO (D4) and TNO (D7) devices. A 10 point adjacent averaging is done to smooth as measured data.

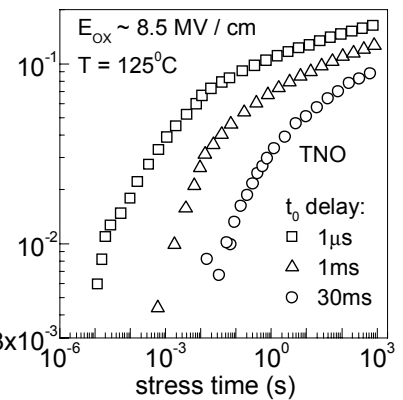
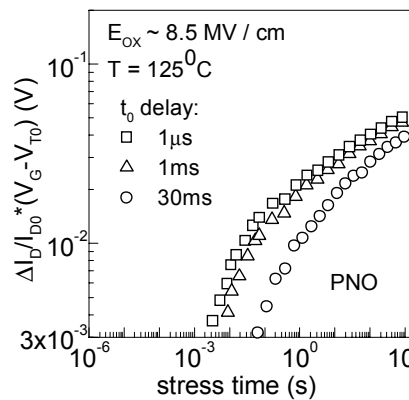


Fig.3. Extracted time evolution of degradation from I_{DLIN} transient of Fig.2, using I_{D0} obtained at different time after application of stress V_G (t_0 delay) for PNO (LHS) and TNO (RHS) devices.

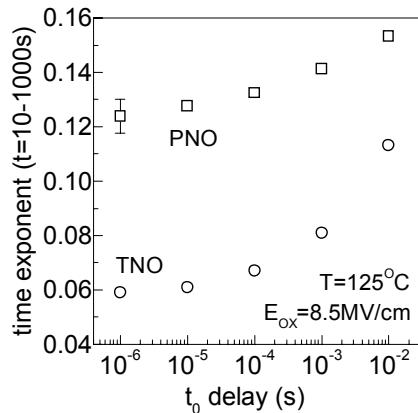


Fig.4. Extracted power-law time exponent (linear fit from 10s to 1000s) for degradation calculated from Fig.2 as a function of t_0 delay for PNO and TNO devices.

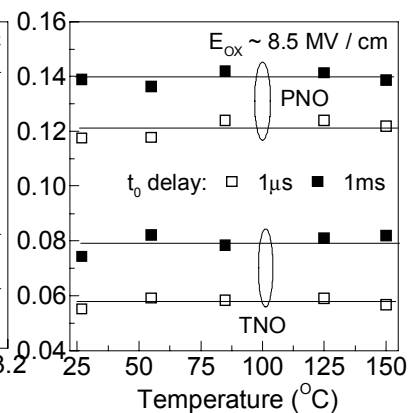
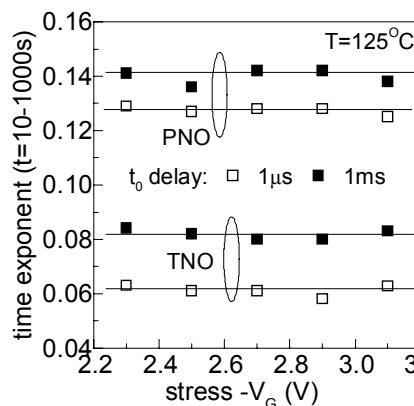


Fig.5. Extracted power-law time exponent (linear fit from 10s to 1000s) as a function of stress V_G (LHS) and T (RHS) for t_0 delay of $1\mu s$ and $1ms$ for PNO and TNO devices (identical to Fig.2). Lines are guide to the eye. Maximum error in time exponent due to noise induced scatter in I_{D0} is ± 0.005 .

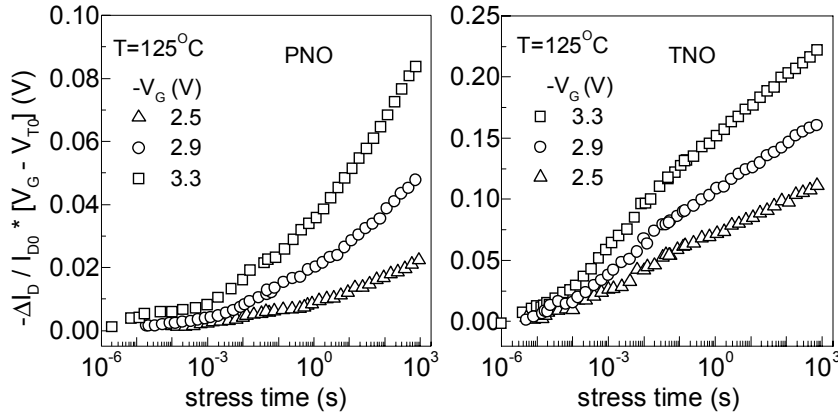


Fig. 6. Time evolution of degradation for different stress V_G plotted in a semi-log scale for PNO (LHS) and TNO (RHS) devices (identical to Fig. 2). Measurements were performed with t_0 of $1\mu s$.

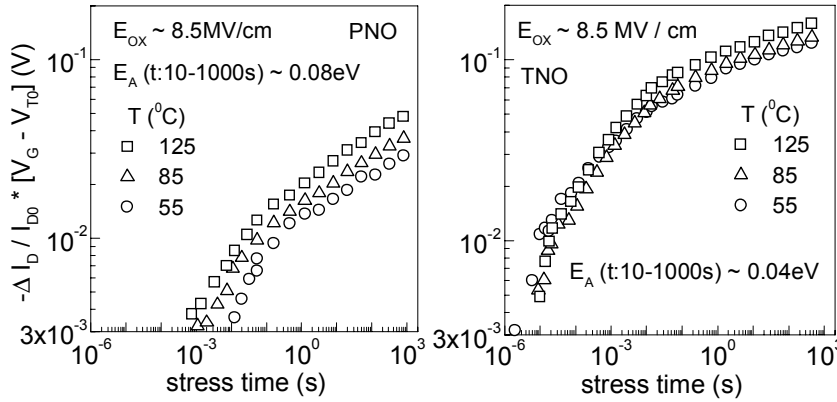


Fig. 7. Time evolution of degradation for PNO (LHS) and TNO (RHS) devices (identical to Fig. 2) at different stress T , measured for t_0 delay of $1\mu s$. Estimated error in E_A is approximately $\pm 0.005 eV$.

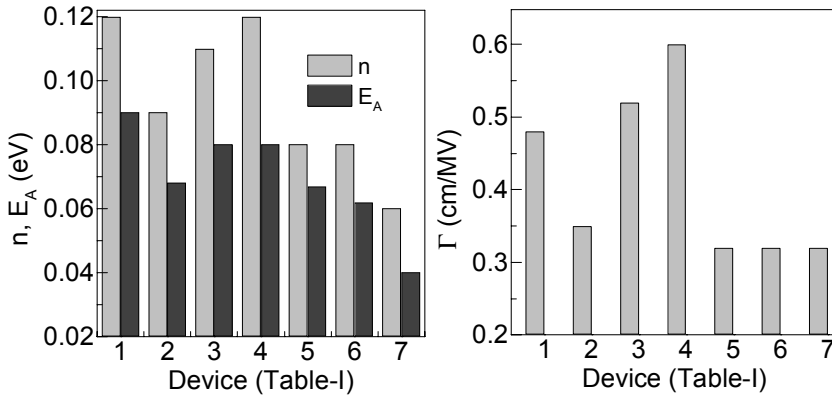


Fig. 9. Material dependence (Table-I) of NBTI parameters: (LHS) power-law time exponent (linear fit from 10s to 1000s) of degradation, activation energy (t : 10-1000s) and (RHS) slope for field dependence (Γ). Obtained n reduces by less than 0.01 for additional 2 decades of stress time. Maximum error in n is ± 0.005 , in E_A is $\pm 0.005 eV$, and in Γ is $\pm 0.02 cm/MV$.

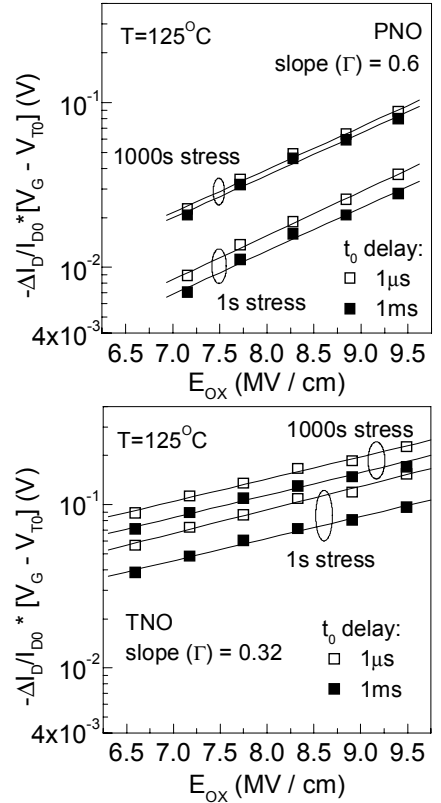


Fig. 8. E_{ox} dependence of degradation for PNO and TNO devices (identical to Fig. 2) measured after 1s and 1000s of stress, for t_0 delay of $1\mu s$ and 1ms. Reported Γ is in cm/MV , with maximum error of approximately $\pm 0.02 cm/MV$.

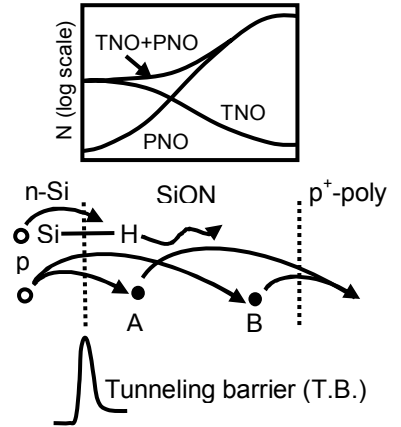


Fig. 10. (Top) Schematic N profile for devices in Table-I, and (Bottom) plausible NBTI physical mechanism. Dashed lines towards LHS and RHS respectively denote Si-SiON and SiON-poly-Si interfaces. A and B denote hole trap positions near substrate and near gate.